Proceedings World Geothermal Congress 2020+1
Reykjavik, Iceland, April - October 2021

The Brimstone Hill Geothermal Prospect, St Kitts: a New Resource Assessment Making Use of coastal Infrared Imaging

Jacques Charroy (1), Sébastien Haffen (1), Yves Géraud (2), Marc Diraison (2), Michel Corsini (3), Marc Munschy (4) and Frédéric Gérard (1)

(1) Teranov SAS, 2 rue du Doyen Marcel Roubault, 54501 Vandœuvre-lès-Nancy, France

(2) Laboratoire Géoressources, 2 rue du Doyen Marcel Roubault, 54501 Vandœuvre-lès-Nancy, France

(3) Laboratoire Géoazur, 250 rue Albert Einstein, 6905 Valbonne, France

(4) Institut de Physique du Globe de Strasbourg, Université de Strasbourg et CNRS, 1 rue Blessig, 67084 Strasbourg, France

jcharroy@teranov.fr, shaffen@teranov.fr, yves.geraud@univ-lorraine.fr, marc.diraison@espe.unistra.fr, corsini@unice.fr, marc.munschy@unistra.fr, fgerard@teranov.fr

Keywords: St Kitts, Brimstone Hill, Geothermal, Resource assessment, Magnetotelluric, Infrared imaging, Thermal flux

ABSTRACT

Teranov has undertaken a full suite of geoscientific surveys of the Brimstone Hill geothermal prospect, located on the western slopes of Mount Liamuiga, the northernmost eruption crater on St Kitts Island in the Lesser Antilles, and north of Brimstone Hill. This work involved a combination of geological, geochemical, and geophysical surveys and, in this paper, we highlight an attempt at perusing surface infrared imaging in order to evaluate heat loss and inform resource assessment results.

The surveys undertaken include a detailed geological survey, two magnetotelluric surveys, a high resolution gravity survey, a drone based aeromagnetic survey, a surface temperature survey using a radiometric sensor carried by UAV, the geochemical analyses of steam-heated boiling spring samples from the crater of the nearby volcano, Mt Liamuiga, of liquid samples acquired 1m below sea level, where waves break and multigas measurements (in-situ gas ratios) of gas seeps. Liquids from a shallow well (9C-23) located near the sea in which temperatures of 51°C had been previously measured were also resampled.

Two magnetotelluric (MT) surveys were undertaken which together highlighted some small dome features in a strongly electrically conductive unit. These features appear to be correlated with the location of N-S faults and are interpreted as showing the locations of preferential upflows along faults. They are interpreted as the marker of hydrothermal alteration above a geothermal upflow, and the base of the conductive zone indicating a temperature of the order of 200-210°C. A resistive body is also clearly apparent below the conductive zone in a NW-SE alignment around Brimstone Hill, and is interpreted to be part of the Brimstone Hill intrusion. The conductive zone wraps around this feature, which indicates that it is likely to act as a heat source to the gas and liquid thermal manifestations observed at the base of Brimstone Hill.

The samples acquired at sea or in the shallow well did not allow for the application of chemical geothermometers with confidence, given that the samples were composed of varying parts of seawater and surface waters, besides the deep geothermal signature. In order to supplement MT interpretations, and potentially identify any overlooked surface thermal features, a drone-borne thermal infrared survey of the vicinity of a known outflow area by the coast was undertaken, which highlighted a wide thermal anomaly at sea along the coastline near Brimstone Hill, centred on the known surface outflow. A method is tentatively applied in an attempt to quantify the heat loss resulting from this outflow.

A conceptual model of the Brimstone Hill prospect is proposed, which is interpreted to host an inferred geothermal resource according to the principles of the Australian Geothermal Reporting Code, 2nd edition. A stored-heat assessment of its power production potential under a binary development scheme was undertaken, which estimates P50 and P90 values of 28MWe and 19MWe, respectively.

1. INTRODUCTION

The Brimstone Hill prospect is located on the western slopes of Mt Liamuiga, in the north of St Kitts island. It has been explored by a number of geoscientific teams including Maury et al. (1990), Geotermica Italiana (1992), Roobol and Smith (2015), and Geonomics. The present work enhances significantly the understanding of the Brimstone Hill geothermal prospect by adding gravity survey results, magnetotelluric sounding results and the outcomes of a thermal infrared survey flown over a part of the coastline in an attempt to identify any leakage of hot fluids at sea, and quantify the heat loss.

As on most Caribbean islands, there is a strong commercial interest in generating electricity from a geothermal source to offset the near total dependence on imported oil for electricity production there, and the high costs associated with it.

2. GEOLOGICAL SETTING

Teranov collaborated with French University laboratories GéoAzur, Géoressources and IPGS to undertake a detailed geoscientific survey of St Kitts Island and of the Brimstone Hill geothermal prospect, located on the western slopes of Mt Liamuiga (Corsini et al (2017a), Corsini et al. (2017b))..

St. Kitts Island is part of the Lesser Antilles volcanic arc, which developed in the eastern part of the Caribbean plate because of the slow, westward subduction of the Atlantic oceanic plate (Figure 1).

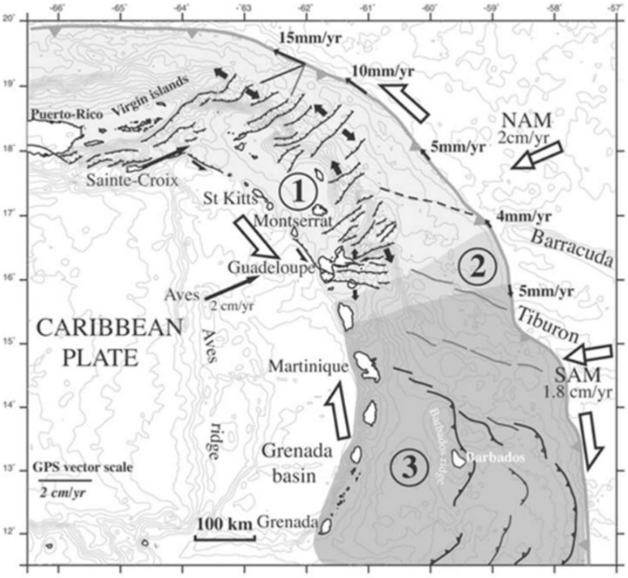

Figure 1: Tectonic model of the Lesser Antilles Arc (Feuillet et al., 2002). Black arrows along the trench: NAM/CAR boundary-parallel slip with rates indicated. 1), in light grey, zone of sinistral extensional shear; 2)- transition zone; 3)- in dark grey, zone of dextral oblique thrusting. (NAM, North American plate; SAM, South American plate; CAR, Caribbean plate).

Mt Liamuiga volcano is the youngest and only active volcano on St Kitts Island, it culminates at 1156m with a date of last eruption estimated at 330 AD +/- 50 years.

The studied area is entirely composed of recent geological formations. The oldest volcanic formations (Mt Liamuiga Series) are volcanic flows and volcano-clastic deposits that outcrop mainly in the summit of the Mt Liamuiga volcano. They are intruded by the andesitic domes of Sandy Point Hill to the north and Brimstone Hill to the south and covered by pyroclastic flows and ash deposits (Steel Dust Series). Four principal families of faults were observed in the field, and confirmed through analysis of the digital terrain model – a LIDAR-derived model with approximately 10m spacing – along the NE-SW, NW-SE, N-S and E-W directions. A map of interpreted and observed faults was built for the area of primary interest (the western slopes of Mt Liamuiga), as shown on Figure 3.

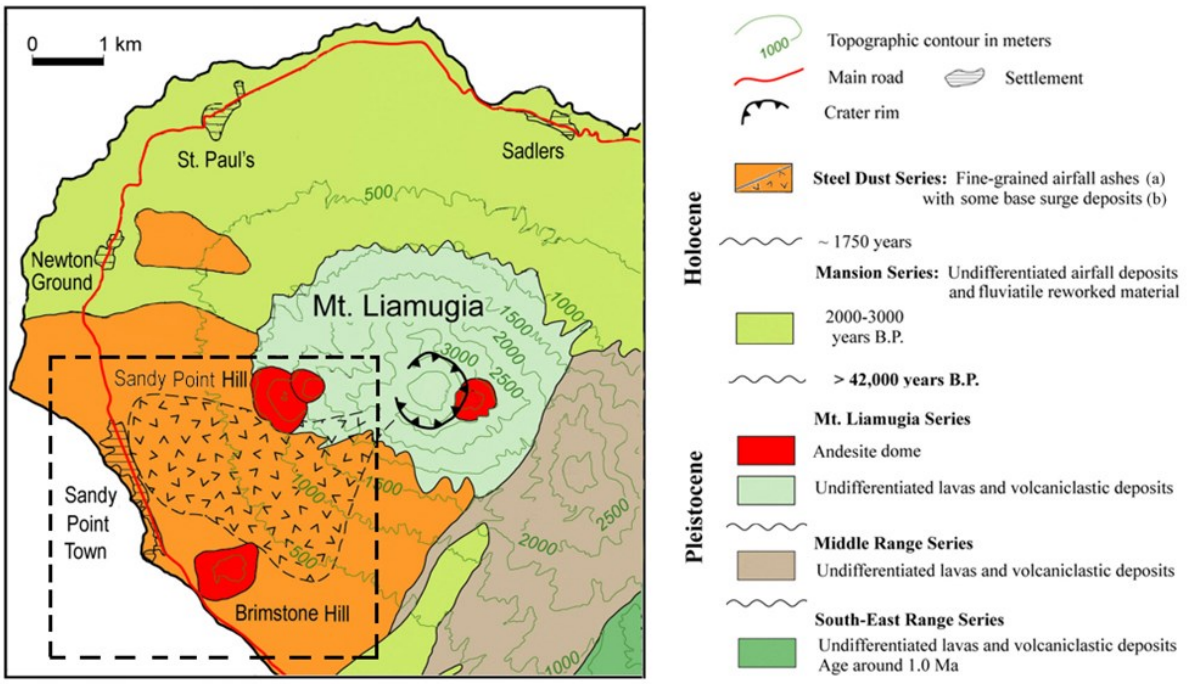

Figure 2: Simplified geological map of the area explored, in Corsini et al. (2017) after Roobol and Smith (2015)

A synthetic structural model was also created on this basis, as seen on Figure 11.

Porosities and permeabilities are thought to be high in the reservoir based on the types of units observed during surveys, the petrophysical measurements undertaken on surface samples and the large number of faults and fractures encountered throughout the prospect area.

Two small craters called Round Hole Crater and Tomba Crater (see Figure 3) are also located in Bourke's Estate, to the north of Brimstone Hill (Corsini et al. (2017a)). These craters are very modest in size, they measure barely one hundred meters in diameter and are about twenty meters deep. Blocks of olivine basalt protrude the walls of both craters and these two craters cut through and expose the Steel Dust Series. They were formed in very recent times, probably after 1624 A.D. (settlement of Europeans in St Kitts), which is in line with the low rate of erosion and infilling observed.

On the periphery of these craters are blocks of basalt, in which magmatic flow is observed and a proof of the nature of their placement in the form of volcanic flow before fragmentation during the formation of the explosion craters. When they are observable, the walls of these craters are nigh-vertical. These walls allow the observation of the volcanic series. These are debris flows with very large andesitic blocks and welded lapillis characteristic of pyroclastic flows (nuées ardentes).

The strong vegetation cover allows only very localized observations which do not allow for a precise definition of the origin of these craters (hydrothermal, phreatic or phreato-magmatic eruption). Only the basalt blocks show the dismantling of a superficial volcanic flow. No explosive breccias were recognized on the periphery or inside the craters.

The topography of St Kitts is very rugged and the thick brush present in some parts of the island makes it difficult to access some areas, even on foot. Mt Liamuiga is located 2-3h walk away from the nearest road access, up steep slopes, which makes the logistics of developing a geothermal power project inside or close to the Mt Liamuiga crater prohibitively complex. For this reason, the low-lying slopes of the island have been the primary exploration target, and the effort expanded to explore beyond the accessible areas into the thick jungle and towards Mt Liamuiga Crater was limited.

3. GEOCHEMISTRY

The surface thermal features of St Kitts were explored and attempts were made at sampling them during two field surveys in April 2016 (Haffen, S. and Gérard, F., 2016) and, with the assistance of IPGP, in July 2016 (Robert, Dessert and Haffen, 2016).

The surface thermal features of St Kitts are grouped in two areas:

- A large 100m by 100m area of surface activity on the northern slopes inside the crater of Mt Liamuiga, which includes fumaroles, solfataras, boiling pools and small mud pools at temperatures reaching up to 96.3°C and at pH values of 2.
- Secondly, a cluster of three areas separated by a few hundred meters, to the west and northwest of Brimstone Hill. It includes an outflow to sea in shallow waters, an old water well which encountered temperatures of 51°C (St Kitts Water Department (1969)), and a carbonate outcrop at the foot of Brimstone Hill from where strong H_2S smells emanate through fractures. Traces of sulphur deposits are present around this gas seep, and in 2017 a temperature anomaly was also detected there (hot gasses, but the low flow did not allow for a good temperature measurement).

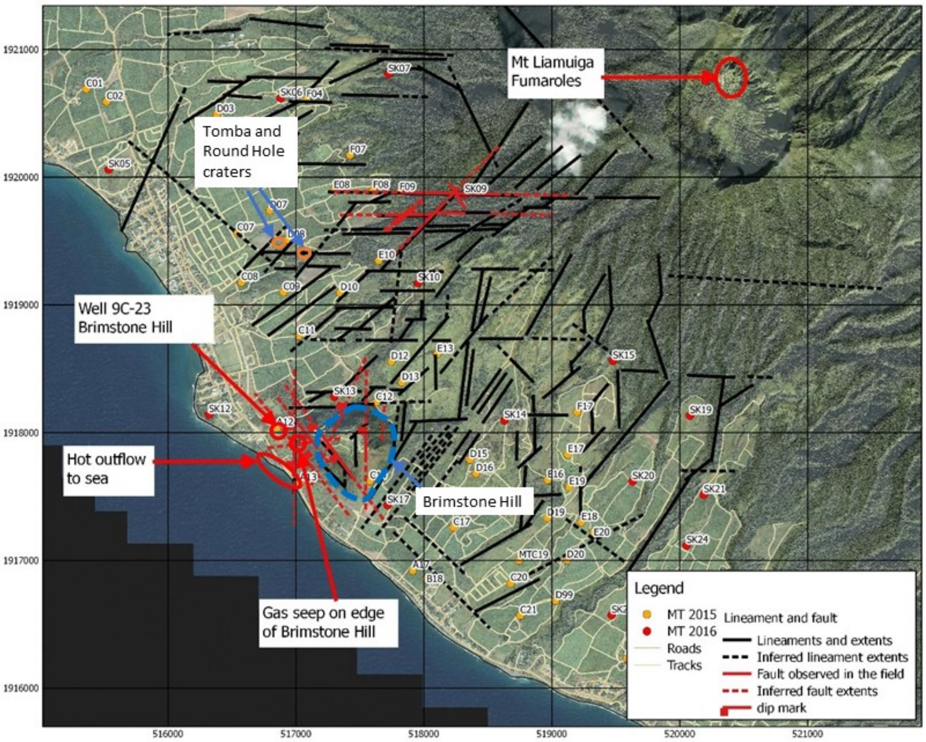

Figure 3: Map of Surface thermal features, faults and lineaments together shown along with the 68 MT stations acquired by Teranov

The acid sulphate composition of the Mt Liamuiga thermal features is an indication of a magmatic character of the fumaroles. A similar, though more dilute character has been reported (Geonomics, 2016) in the well bore waters of well 9C-23 Brimstone Hill.

No direct indication of temperature of the deep reservoir exists at Brimstone Hill, however gas geothermometry results applied to 3 uncontaminated Giggenbach flask samples obtained on Mt Liamuiga indicate a temperature of 212°C in the deep reservoir Figure 4).

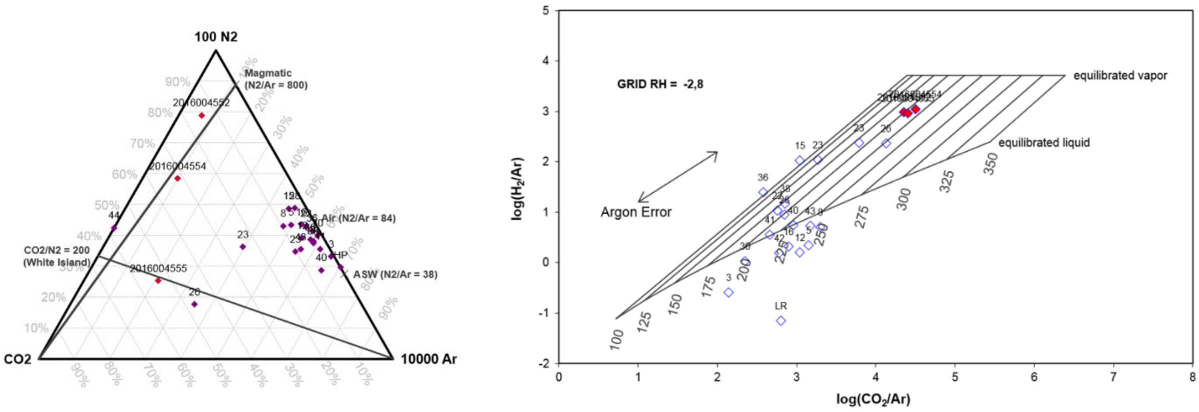

Figure 4: Left: ternary plot showing the 3 valid gas samples acquired at St Kitts (in red) compared with the graph of sample measurements from other geothermal prospects around the world. Right: H_2/CO_2 gas geothermometer yields a deep reservoir temperature estimate of 212°C (dots in red combined with measurements from other geothermal systems worldwide)

No geothermometry measurements are present for the geothermal system of primary interest, associated with the surface thermal features north of Brimstone Hill. Both the fumaroles and the well samples have been interpreted as having a magmatic component, so it is likely that the heat sources for the two thermal areas are common at depth. As a result, we assume the same value of temperature obtained from the gas geothermometry results at Mt Liamuiga crater for the Brimstone Hill prospect.

4. GEOPHYSICAL SURVEYS AND THERMAL IMAGING

4.1. Gravity survey

A gravity survey was undertaken by LM consulting (2016), which yielded very good quality data (repeatability better than 20µgal), and showed a low amplitude of variation (3.4mgal) over the area explored, except at Brimstone Hill. This confirms that Brimstone Hill does have a strongly contrasting (lower) density than the surroundings, while these densities are generally rather homogeneous over large depth intervals. This is inferred from the low gravity survey amplitude and the extensive faulting observed with little associated gravity signature.

A Bouguer anomaly map of the survey results for a density of 2.8 was produced based on this dataset (Figure 5) after applying the Nettleton method to determine the optimal density for this purpose.

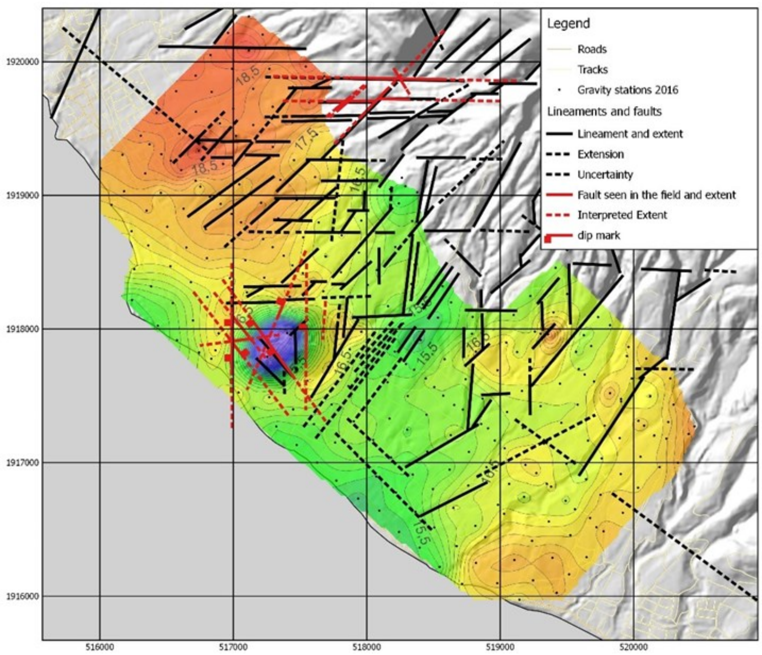

Figure 5: Map of the complete Bouguer anomaly computed with a density of 2.8g/cc, shown superimposed on fault and lineament structures.

Bouguer anomaly contours are rather difficult to interpret and not clearly correlated with the fault structures observed from geological interpretations, with the exception of a good alignment between the major SW-NE fault that crosses the crater and an apparent gravity interface.

The general lack of correlation between bouguer anomaly contours and structural interpretations is interpreted to be due to the fact that density variations are indeed low and volcanic materials, of a homogeneous density over a large depth interval, which entails small amplitude in Bouguer anomaly values at surface, even in the presence of intense faulting.

It is apparent that fault placements cannot be accurately determined on the basis of gravity results in this case.

4.2. Magnetic survey

An aeromagnetic survey was undertaken over the area of the Brimstone Hill geothermal prospect, using a fluxgate magnetometer carried by a DJI Matrice 100 UAV, see Munschy et al (2016).

The majority of measurements were carried out with a line spacing of 100m and an altitude of 100m. A limited area was also surveyed with a reduced line spacing and height of 25m in the immediate surroundings of Brimstone Hill. A reduction to the pole was undertaken on the 100m data to assist interpretation (Figure 6).

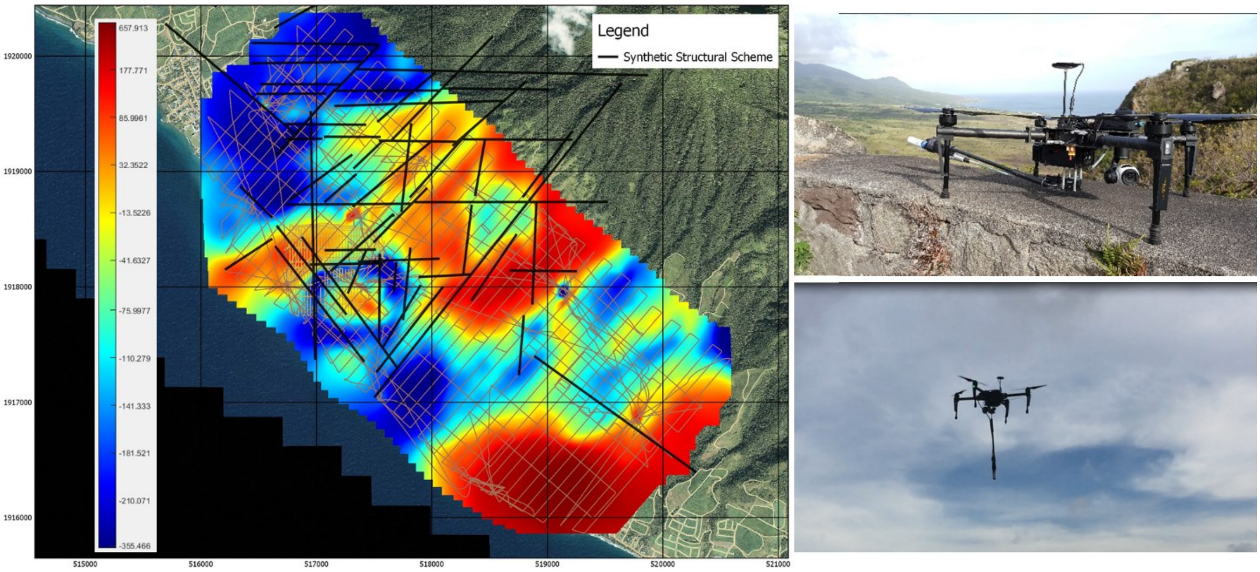

Figure 6: Map of total magnetic intensity reduced to the pole based on 100m height UAV flight lines (left). The flight lines shown in brown include 100m spaced lines acquired 100m above topography and 25m spaced lines on Brimstone Hill and to the North and West of it. The interpreted structural model is superimposed on the magnetic anomaly map. On right: DJI Matrice 100 UAV equipped with the IPGS/DIEFI gear and fluxgate magnetometer (Munschy et al., 2016).

A clear magnetic anomaly coincides with the Brimstone Hill intrusive. It appears to be close to symmetrical.

A magnetic high is present to the south of the area explored, but its boundaries are not clearly defined.

A clear and low frequency magnetic low is also present to the north-east of Brimstone Hill along the length of the main SW-NE fault. The mapped faults in this area have no visible magnetic signature.

There is good agreement between the structural model (in particular the SW-NE trending interpreted faults) and some linear features shown on the aeromagnetic map. The observed NW-SE faults, on the other hand, have no observable magnetic signature.

4.3. Magnetotelluric surveys

Two MT surveys were undertaken and the resulting data was inverted in 1D and 3D (Imagir (2016a, b, c)). The resulting models were interpreted jointly in an attempt to delineate the base of the conductive zone (see Figure 7-7). Some areas (front of Brimstone Hill) had particular quality issues which are apparent on 1D models, and where 1D and 3D inverted results diverge strongly. In these cases, a choice was made for the interpreted base of the conductor to follow more closely one set of models over the other depending on the dimensionality of each sounding.

The results highlight some near-surface conductive features with an intricate geometry, which seems to wrap around an underlying resistive body and also exhibit a slight dome shape (Figure 9). These features appear to be correlated with the location of N-S faults and are interpreted as showing the locations of preferential upflows along faults. They are interpreted as the typical marker of hydrothermal alteration above a geothermal upflow, and the base of the conductive zone indicating a temperature of the order of 200-210°C.

The resistive body below it is clearly delineated in a NW-SE alignment around Brimstone Hill, and is interpreted to be part of the Brimstone Hill intrusion. The fact that the conductive zone wraps around this feature is interpreted as a sign of its acting as a heat source to the gas and liquid thermal manifestations observed at the base of Brimstone Hill, in a NS alignment.

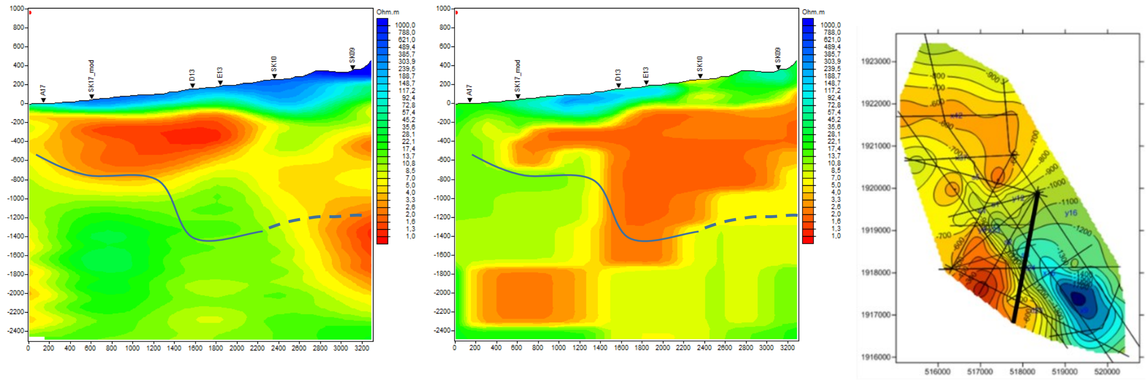

Figure 7: 1D modelled MT cross section (left) and 3D modelled MT cross section (middle) along profile s3 (south at left). The interpreted elevation contours of the base of the conductor are shown on the right.

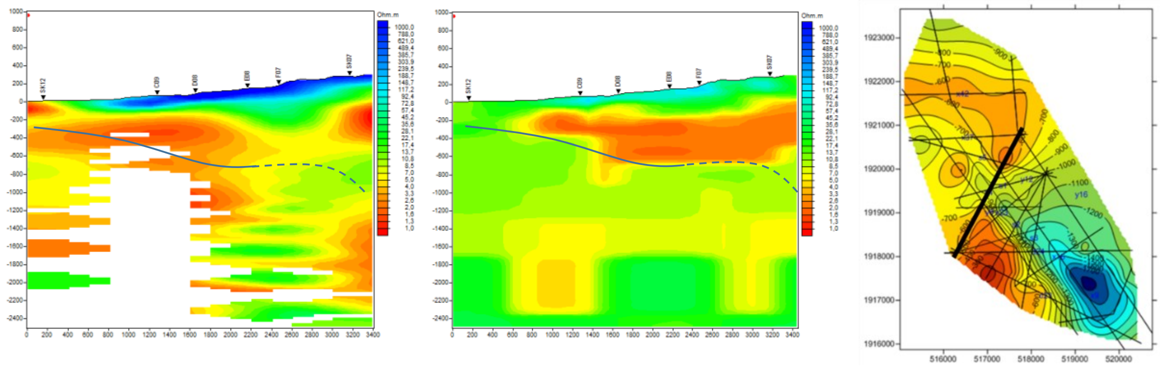

Figure 8: 1D modelled MT cross section (left) and 3D modelled MT cross section (middle) along profile s4 (SW at left). The interpreted elevation contours of the base of the conductor are shown on the right.

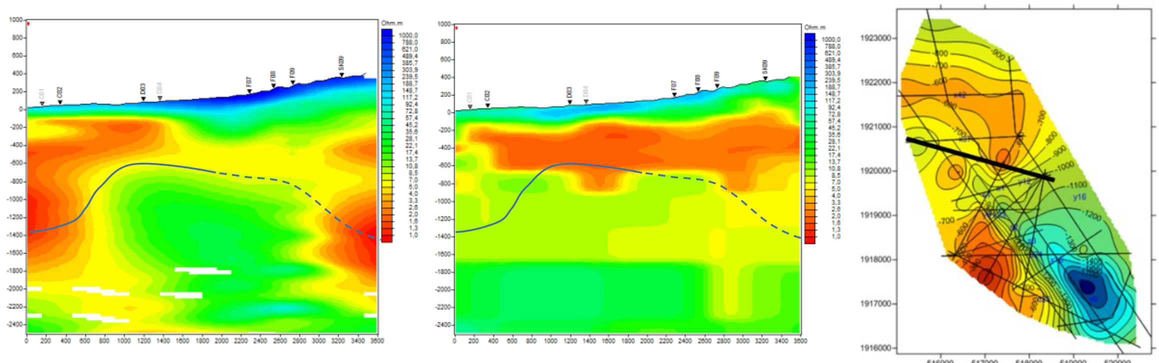

Figure 9: 1D modelled MT cross section (left) and 3D modelled MT cross section (middle) along profile s5 (WNW at left). The interpreted elevation contours of the base of the conductor are shown on the right.

4.4. Thermal infrared imaging

A drone-borne infrared survey of the geothermal system was also undertaken, which highlighted a wide zone of thermal anomaly along the coastline near Brimstone Hill, centred on the known surface features. An assessment was made of the thermal energy expanded from cooling such an anomaly, which yielded a value of heat flow of 8MWth, which is significant. The method used is very sensitive to parameters such as wind speed and thickness of the cooling layer, so this value has a high uncertainty until more measurements can be undertaken on different days with different wind conditions.

In order to evaluate the intensity of the outflow to sea, and be able to quantify the corresponding heat flux, Teranov requested a drone based aerial survey of this coastal area. This was undertaken by Drone Alsace in July 2016 using an eBee drone and a calibrated radiometric sensor in the thermal infra-red band (7.5-13μm). The survey was run in less than perfect conditions as logistics didn't allow it to happen at dawn. As a result, the land part of the survey shows very high temperatures along roads and man-made infrastructure.

However, measurements at sea showed a very clear thermal anomaly of approximately 2°C amplitude coinciding with the location of the outflows and extending widely laterally and out to sea (see Figure 10), the extent of the anomaly being approximately 430m long by 90m wide, covering an area of 18000m2.

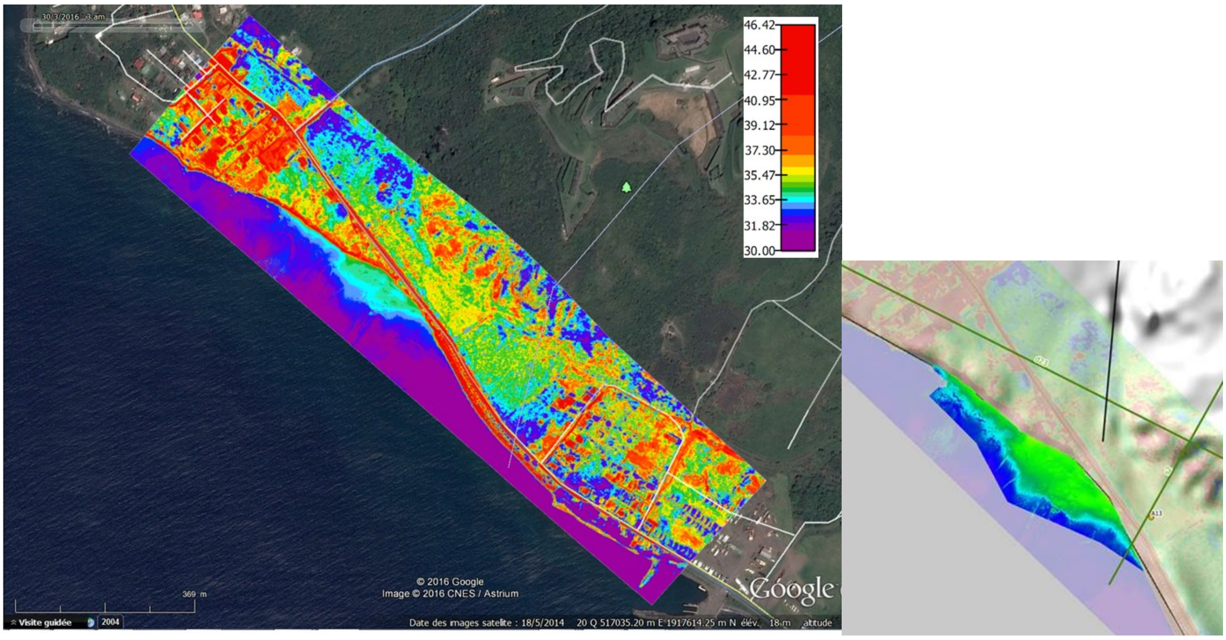

Figure 10: Infrared thermography survey results showing temperatures computed in °C, and the results with approximate lateral limits of the temperature anomaly.

Recent studies on thermal exchanges by convection between the surface of a body of water and atmosphere have shown the existence of an empiric relationship between the surface thermal flux and the intensity of thermal convection in water in calm weather conditions (without wind) and with winds strong enough to create turbulence in water (Conover and Saylor (2007) ; Garrett et al. (2013)). Conover and Saylor measure the convection intensity through the standard deviation of temperatures calculated on an infrared image in either calm or windy conditions. They show experimentally that they can retrieve in this way the relationship between thermal flux and the standard deviation of temperatures σ established by Businger (1973):

$$\sigma = \left(\frac{q}{\rho_w\, c_{pw}\, u_*}\right)^{2/3} \left(\frac{\Theta}{gh}\right)^{1/3} \tag{1}$$

where ρ_w and c_{pw} are the density of sea water (1,025 kg/m3 at 30ºC) and its specific heat capacity at constant pressure (4.011 KJ/kg.K), u* is the wind speed (from 1 to 7 m/s), Θ is the mean temperature of surface water, g is the acceleration of gravity (9.81 m/s2), and h is the height of the water column. From this equation, a relationship can be derived to calculate surface thermal flux q based on the standard deviation of surface temperatures σ :

$$q = \rho_w\, c_{pw}\, u_* \left(\frac{g\, h\, \sigma^3}{\Theta}\right)^{1/2} = \beta\, u_*\, h^{1/2}\Theta^{-1/2}\sigma^{3/2} \tag{2}$$

where β is the equivalent of a heat transfer coefficient (12876900 W.m^{-2}. K^{-1}).

Table 1: Surface Thermal flux and total thermal cooling flow evaluated based on the convective cooling of a convective body of water

σ	u*	Θ	h	q	S	Φ
K	*m.s^{-1}*	*K*	*m*	*W.m^{-2}*	*m^2*	*MWth*
0.002	7	303.15	1	463	18,000	8.3

A total cooling flow of 8.3MWth is thus interpreted to exit the shallow reservoir as a result of the sum total of outflows to sea from the coastal surface thermal features. The applicability of this formula remains however to be tested in a controlled environment to enable calibration, and verify that it can indeed be applied with similarly small temperature differences. We thus consider this an interim result, needing more work to be confirmed. Regardless of the question of applicability to the conditions, the result is likely to contain a large uncertainty. Ideally a number of repeat measurements should be undertaken to ascertain the results, with acquisition in different wind conditions, and at various times of the day. The order of value seems however realistic given the large extent of the anomaly observed. The wind speed was of the order of 8.3m/s, so that we used the maximum bound of validity (7m/s) of the formula instead. Prof. Jean-Jacques Royer is gratefully acknowledged for providing assistance with a-priori validation of the heat flux derivation method applied here.

5. CONCEPTUAL MODEL AND RESOURCE ASSESSMENT

5.1 Conceptual Model

A conceptual model was built on the basis of the geoscientific data presented herein (Figure 11 and Figure 12). It includes a deep liquid geothermal reservoir intimately associated with the network of large SW-NE faults that dominate the structural grain of St Kitts. We interpret that this reservoir is fed by fluids heated at depth by the volcanic chimney of Mt Liamuiga and its branches, one of which being the intrusion that generated Brimstone Hill.

There appears to be a concentration of signs of upflow along NS aligned faults between Brimstone Hill and the Tomba / Round Hole craters and beyond, and also in the immediate vicinity of the Brimstone Hilll intrusive. Given the interpreted link between the heat source of the Mt Liamuiga fumaroles and the prospect, we have used gas thermometer analysis based on analysis of these features to assess the temperature of the fluids in the reservoir, at 212°C. We acknowledge that the lack of liquid surface thermal features coming directly from the resource implies some uncertainty remains on this estimate of temperature in the reservoir. The area of the resource was interpreted to be 3.8km2 (red outline on Figure 11) based on MT results.

Extensive matrix and fracture permeability and porosity are interpreted to exist in the reservoir, with the features controlling the resource appearing to follow a NS direction, and upflows located along these faults and along the areas showing the small dome features described earlier.

A large part of the recharge of the geothermal field is interpreted to come from the sea, which would provide good pressure support to the geothermal reservoir at depth. Recharge from meteoric waters is considered to add only a small contribution to reservoir recharge due to the widespread low resistivity (potentially impermeable) cover encountered in the area explored.

The lateral boundaries of the system appear relatively well closed in all directions except to the north, where the conductive zone tapers off.

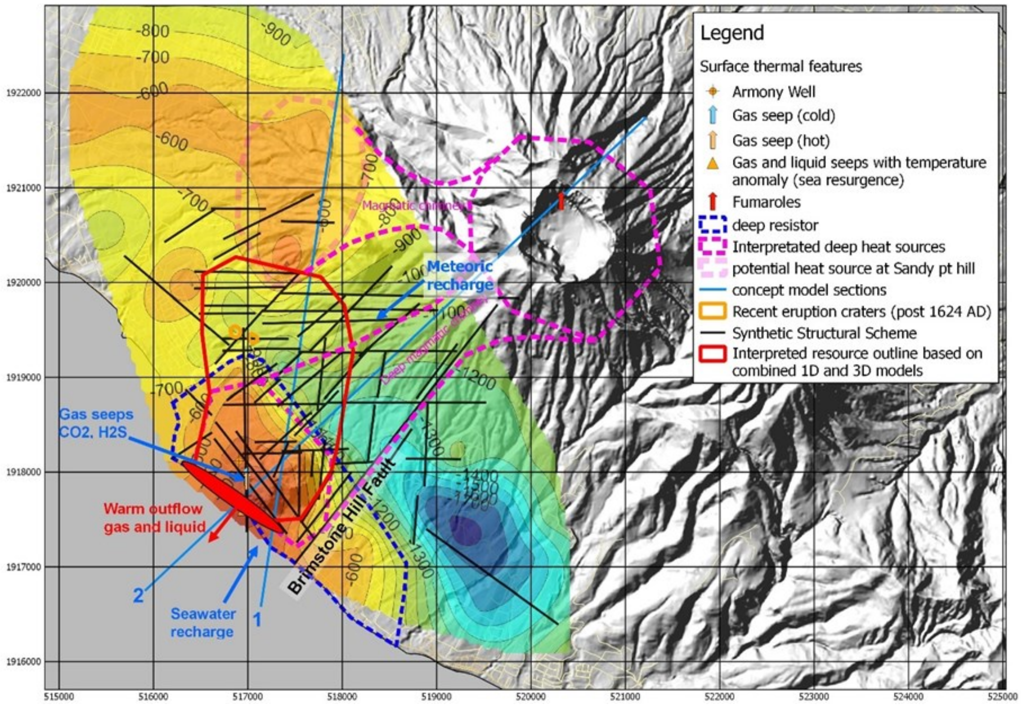

Figure 11: Conceptual model map for the Brimstone Hill Geothermal System showing the relief in the elevation of the base of the conductive zone on the basis of 1D models (in masl).

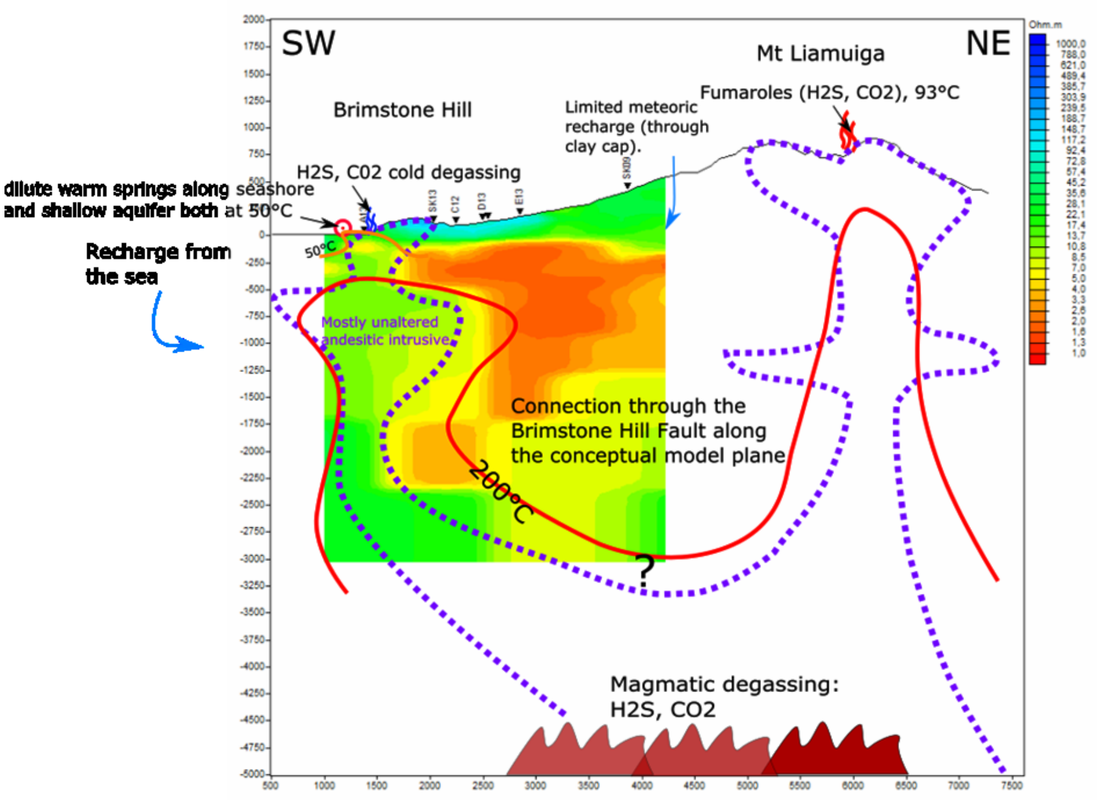

Figure 12: Conceptual model cross-section along profile 2 (cf Figure 11)

5.2 Assessment of power production potential

Given the geoscientific information available to this point, we interpret that an inferred geothermal resource is present with temperatures in excess of 200°C within the red outline on Figure 11, which could be suitable for the production of electricity using a binary plant.

An estimate of power production potential for a binary power plant was then produced using the stored heat method and a probabilistic assessment of input variables (Monte-Carlo model). This assessment was made following the principles of the Australian Geothermal Resources and Reserves Reporting Code, 2nd Edition (2010). The results indicate that the Brimstone Hill inferred resource has a 50% probability of being able to support a 28MWe binary plant (P50), and a 90% probability of being able to support a 19MWe binary plan (P90). The input parameters used in this calculation are given in Table 2 below.

Table 2: Input Parameters of Stored Heat Energy Assessment

Parameter	Bound	Unit	Value
Resource Area (fixed value)	Fixed value	km²	3.7
Resource Thickness	Minimum	m	800
	Most Likely Value	m	1000
	Maximum	m	1500
Porosity	Minimum	%	5
	Most Likely	%	10
	Maximum	%	12
Temperature	Minimum	°C	180
	Most Likely	°C	212
	Maximum	°C	230
Rock Density	Assumed	kg/m^3	2700
Liquid Saturation in reservoir	Assumed	%	100
Rock Specific Heat Capacity	Minimum	kJ/kg°C	0.927
	Most Likely	kJ/kg°C	0.942
	Maximum	kJ/kg°C	0.950
Recovery Factor (uniform distribution)	Lower Bound	%	8
	Higher Bound	%	16
Net Conversion Efficiency (including 10% power plant losses)	Minimum	%	12.6
	Most Likely	%	15.1
	Maximum	%	16.5

Parameter	Bound	Unit	Value
	Correlation Used	-	SKM (Reservoir Temperature Dependent), AGRCC 2010b

CONCLUSIONS

The geoscientific understanding of the Brimstone Hill prospect was significantly advanced by the results of the MT, gravity, magnetic and thermal imaging surveys undertaken at and around it. A conceptual model was proposed in which intrusive bodies linked at depth with the Liamuiga volcanic plumbing are providing a principal heat source feeding the geothermal activity observed at surface, and are most likely responsible for the small eruptions that led to the creation of the Tomba and Round Hole Craters in relatively recent (historic) times.

The North-South faults extending between Brimstone Hill and these craters are interpreted to control some of the upflow. Indices of elevated prospectivity in a particularly conductive shallow and thin conductor are observed along this axis. On this basis, and that of an alignment of surface thermal features in the same direction, we delineated an area considered most prospective for a geothermal development, which we interpret constitutes an inferred geothermal resource according to the principles of the Australian Geothermal Reporting Code, 2nd edition. Our assessment of this inferred resource is that it has 50% probability of being able to support a 28MWe binary plant, and 90% probability of being able to support a 19MWe binary plant.

An estimate of heat loss from the reservoir into the sea via a well-known surface outflow was also undertaken using thermal infrared imaging and a promising method which will need some testing and calibration in a controlled environment before it can be safely applied to a case such as ours, where temperature differences between anomaly and background are low. This technique should be considered of interest for quantifying shallow outflows to sea.

REFERENCES

AGRCC: The Geothermal Reporting Code, Second edition (2010a).

AGRCC: Geothermal Lexicon for Resources and Reserves Definition and Reporting, Edition 2, (2010b).

Baker, P.E.:. Volcanic hazards on St Kitts and Montserrat, West Indies. Journal of the Geological Society, London (142), 279-295 (1985).

Businger, J. A.: A note on free convection. Bound.-Layer Meteor., 4, 323–326 (1973).

Conover, T. A., and J. R. Saylor: Statistics of the surface temperature field of an air/water interface under air flow. Exp. Fluids, 43, 509–524 (2007).

Corsini, M., Diraison, M., Gérard, F., Haffen, S. and Walter, B.: St. Kitts Structural Synthesis including contributions from supplementary geological and geophysical studies, report to Teranov (2017a)

Corsini, M., Diraison, M. and Haffen, S.: Geological study of St Kitts island, Geological report for Teranov v2 (2017b).

Feuillet, N., Manighetti, I., Tapponnier, P. and Jacques, E.: Arc parallel extension and localization of volcanic complexes in Guadeloupe, Lesser Antilles. Journal of Geophysical Research: Solid Earth, 107(B12) (2002).

Garrett A.J., Kurzeja R.J., Villa-Aleman E., Bollinger J., Pendergast M.: Remote Measurement of Heat Flux from Power Plant Cooling Lakes, Journal of Applied Meteorology and Climatology, 52, 1366-1378 (2013).

Geonomics: Geophysical and geothermometer of the geothermal resource St Kitts, Report prepared for Teranov (2016).

Geotermica Italiana: Exploration for geothermal resources in the Eastern Caribbean: Final Report, Contract TCD CON 15 (1992).

Haffen, S. and Gerard, F.. Résurgences hydrothermales naturelles, St Kitts, Avril 2016: Mesures de temperatures et échantillonages de fluids, Teranov report (2016).

Imagir: Traitement des données magnétotelluriques St Kitts (St Kitts and Nevis), data processing report to Teranov (2016a).

Imagir: Magnetotelluric data – St Kitts, new survey (April 2016). Presentation to Teranov (2016b).

Imagir: 3D Inversion of Magnetotelluric data, Saint Kitts, final report to Teranov (2016c).

L.M Consulting: Exploration d'un gisement géothermique de haute temperature, Mt Liamuiga / Brimstone Hill, St Kitts, Campagne de mesures de gravité, Rapport de synthèse des mesures gravimétriques (2016)

Maury, R. C., Westbrook, G. K., Baker, P. E., Bouysse, P. and Westercamp, D.: Geology of the Lesser Antilles. The Caribbean Region, 141-166 (1990).

Munschy, M., Gavazzi, B., Galluser, F. and Freville, T.: Cartographie magnétique en drone DJI Matrice 100, Saint Kitts – Basse Terre, 27 juin au 5 Juillet 2016, UAV aeromagnetic survey report to Teranov (2016).

Robert, V., Dessert, C. et Haffen, S.: Rapport technique – mission à St Kitts des 5 et 6 juillet 2016, report to Teranov (2016).

Roobol M. J. and Smith A. L.: Geological map of St. Kitts, West Indies (2015)

Ussher, G., Harvey, C., Johnstone, R., Anderson, E.: Understanding the resistivities observed in geothermal systems, Proc. World Geothermal Congress 2000, Kuyshu-Tohuku, May 28th-June 10th, Japan (2000).

St Kitts Water Department: Drilling notebook #2 for period 1969-1970, referencing well 9C-23 Brimstone Hill (1969).